Power control of ultra-wideband optical communication system based on optimization algorithm

ZHU Xingyu*[a], ZHOU Jing[a], YU Changyuan[a]
[a] Dept. of Electrical and Electronic Engineering, The Hong Kong Polytechnic University, 11 Yuk Choi Road, Hung Hom, Kowloon, Hong Kong

ABSTRACT

In order to address the challenges brought by high bandwidth requirements to optical communication networks and improve the capacity of ultra-wideband wavelength division multiplexing systems, an optical power optimization algorithm based on the marine predator algorithm is used to optimize the launched power to achieve the goal of maximizing channel capacity. At the same time, the maximum capacity strategy, high and flat capacity strategy, and flattest capacity strategy are applied to meet different transmission requirements, achieving a balance between capacity and ripple. The simulation results show that compared with the brute force search method, the marine predator algorithm-based optimization algorithm significantly reduces the optimization time required and achieves advantages in both total capacity and ripple flatness. This method can be used to quickly optimize optical network design before actual deployment.

Keywords: Ultra-wideband Wavelength Division Multiplexing, Optical Communication Networks, Optimization Algorithms, Marine Predator Algorithms

1. INTRODUCTION

1.1. Background

The deployment of the fifth generation (5G) mobile communication system and the advent of the big data era have brought tremendous development to fields such as streaming media platforms and cloud computing, but the requirement for high bandwidth also poses challenges to the communication network. The continuous growth of network traffic demand has prompted modern optical communication networks to further improve their transmission capabilities. In order to achieve this goal, researchers mainly strive in two feasible directions: (a) Space Division Multiplexing (SDM) [1], which can be achieved using multi-core fibers (MCF) or multi-mode fibers (MMF), or (b) Ultra-Wideband Wavelength Division Multiplexing (UWB-WDM) systems [2], which will utilize a larger spectral portion of the fiber to improve transmission capabilities. The SDM solution has great potential to increase transmission capacity, but it requires significant modifications to existing optical transmission systems, design and deployment of new fibers and equipment, which results in significant cost investments. Compared to other solutions, UWB-WDM can utilize existing fibers and equipment, but it maximizes the utilization of multiple bands. This feature makes it the most feasible short-term solution to increase the capacity of optical network systems. Some research results have addressed the commercial solutions of UWB-WDM systems in the C+L band [3-5], taking into account the effects of amplified spontaneous emission (ASE), nonlinear interference (NLI), and stimulated Raman scattering (SRS), and thus defining the generalized signal-to-noise ratio (GSNR) as a parameter for quantifying the specified optical path quality of transmission (QoT) [6, 7]. In [8], a channel capacity of 94.9Tbps was achieved in 1900km of C+L band transmission, while in [9], a capacity of 150.3Tbps was achieved in 272

Optoelectronic Devices and Integration XIII, edited by Xuping Zhang, Baojun Li, Changyuan Yu, Xinliang Zhang, Proc. of SPIE Vol. 13236, 132360F
 · 0277-786X · doi: 10.1117/12.3035357

channels over 40km of C+L+S band transmission.

In order to improve the overall transmission capacity of the system, it can be considered to optimize the power allocation of the channel. However, the increase in computational complexity brought about by GSNR and multi span transmission is difficult to avoid. To improve computational efficiency, the Gaussian noise model (GN model) and its closed-form approximation proposed in [10] and [11] are widely used, which has a significant effect on simplifying the calculation of NLI noise and SRS. Especially in systems with bandwidths below 15THz, its calculation of Raman gain distribution can greatly reduce the computational complexity of SRS. Meanwhile, a scheme called local optimization leads to global optimization (LOGO) to some extent solves the optimization problem of multi span transmission [12]. The LOGO scheme indicates that optimization on one span can determine the overall optimization of the system. Therefore, the optimization process of multi span transmission systems can be achieved by considering the performance of one transmission link, which greatly reduces the computational complexity of real systems.

Using iterative search to optimize the function in a given search domain is a simple optimization solution, which achieves power control on the C+L+S band in [13]. In this work, the power distribution of the band is assumed to be flat, which can achieve the high-capacity recording achieved in [9]. However, considering the impact of SRS, relying solely on a flat launched power to achieve optimal capacity will result in larger ripples at the receiving end, which will have a significant impact on user experience. If each band is considered separately, introducing the center frequency power and power slope offset of the band can to some extent solve this problem. If a suitable search domain is defined for these two parameters, and a certain step size is used to search for these two parameters in each band, it can approach the optimal overall capacity to the greatest extent possible, this scheme is referred to as brute-force searching (BFS) in [14]. However, it is obvious that this process is time-consuming, especially in actual network planning. Therefore, an algorithm called the Marine Predator Algorithm (MPA) was applied in this study, which has been proven to have good performance in large-scale optimization and avoiding local optima [19]. We will apply two algorithms separately to control the power of UWB-WDM systems and compare their performance.

2. METHODOLOGY

2.1. Noise analysis in UWB-WDM Systems

a. Nonlinear noise

The nonlinear noise in UWB-WDM system is calculated by Equation 1:

$$P_{NLI} = \eta_n P_i^3 \tag{1}$$

Where P_i is the input power of channel of interest i, η_n is the fiber nonlinear coefficient after n spans, which is composed of self-phase modulation (SPM) and cross-phase modulation (XPM),

$$\eta_n(f_i) \approx \sum_{j=1}^{n} \left[\frac{P_{i,j}}{P_i}\right]^2 \cdot \left[\eta_{SPM,j}(f_i) n^{\epsilon} + \eta_{XPM,j}(f_i)\right] \tag{2}$$

Where $\eta_{SPM,j}(f_i)$ is the SPM contribution and $\eta_{XPM,j}(f_i)$ is the total XPM contribution after j spans, $P_{i,j}$ is the power of COI i launched into the j span and P_i is the launch power of COI i. The closed-form approximation of GN model was used to calculate the SPM and total XPM contribution [15], the closed-form approximation for the SPM contribution is

$$\eta_{SPM}(f_i) \approx \frac{4}{9}\frac{\gamma^2}{B_i^2}\frac{\pi}{\phi_i\bar{\alpha}(2\alpha+\bar{\alpha})}\cdot\left[\frac{T_i-\alpha^2}{a}\operatorname{asinh}\left(\frac{\phi_i B_i^2}{\pi a}\right)+\frac{A^2-T_i}{A}\operatorname{asinh}\left(\frac{\phi_i B_i^2}{\pi A}\right)\right] \tag{3}$$

With $\phi_i = \frac{3}{2}\pi^2(\beta_2 + 2\pi\beta_3 f_i)$, $A = \alpha + \bar{\alpha}$ and $T_i = (\alpha + \bar{\alpha} - P_{tot}C_r f_i)^2$. The closed-form approximation for the total XPM contribution is

$$\eta_{XPM}(f_i) \approx \frac{32}{27}\sum_{k=1,k\neq i}^{N_{ch}}\left(\frac{P_k}{P_i}\right)^2\frac{\gamma^2}{B_k\phi_{i,k}\bar{\alpha}(2\alpha+\bar{\alpha})}\cdot\left[\frac{T_k-\alpha^2}{\alpha}\operatorname{atan}\left(\frac{\phi_{i,k}B_i}{\alpha}\right)+\frac{A^2-T_k}{A}\operatorname{atan}\left(\frac{\phi_{i,k}B_i}{A}\right)\right] \tag{4}$$

With $\phi_{i,k} = 2\pi^2(f_k - f_i) + [\beta_2 + \pi\beta_3(f_i + f_k)]$.

b. Analysis of SRS and ASE noise in optical amplifiers

In UWB-WDM systems, the accumulation of SRS in the system will cause power to shift from high frequency to low frequency, thereby further affecting the power distribution of NLI noise and ASE noise. For non-flat launched power spectral density (PSD), the gain of SRS can be represented in closed form approximate [16, 17],

$$G_{SRS}(f_k) = \frac{P_{tot}e^{-f_k\cdot C_r L_{eff}P_{tot}}}{\sum_l P(f_k)e^{-(f_k-f_l)C_r L_{eff}P_{tot}}} \tag{5}$$

where C_r is the Raman gain slope, L_{eff} is the fiber effective length and is defined as $L_{eff} = \frac{1-e^{-\alpha z}}{\alpha}$, P_{tot} is the total launch power. By deriving a simple formula, the difference in outer channel power transmission under uniform launched power can be calculated as

$$\Delta\rho(z)[dB] = 4.3\cdot P_{tot}C_r L_{eff}B \tag{6}$$

It can be observed that when the fiber parameters are determined, the difference in power transfer is only related to the total launch power and total channel bandwidth. After 80km of transmission in the C-, L-, and S- bands, different uniform transmission powers are affected by the SRS gain, as shown in Figure 1. The power at the receiving end will show a clear trend of shifting from high frequency to low frequency.

Moreover, SRS will further affect the ASE noise of the optical amplifier (OA). In different channels, the gain required by OA needs to consider SRS, which can be expressed as [18],

$$G_{OA}(f) = e^{\alpha(f)\cdot L_s}\cdot G_{SRS}^{-1}(f) \tag{7}$$

Where $\alpha(f)$ is fiber loss parameter depend on channel center frequency f and L_S is the length of fiber span. From this, the ASE noise of OA can be calculated,

$$P_{ASE} = hf\cdot NF(f)(G_{OA}(f) - 1)B_{ch} \tag{8}$$

with h represents the Planck constant, B_{ch} represents the bandwidth of the channel, $NF(f)$ is the frequency dependent noise figure of the OA. Therefore, the gain provided by OA will not be a flat value, and the ASE noise will also be a frequency dependent value.

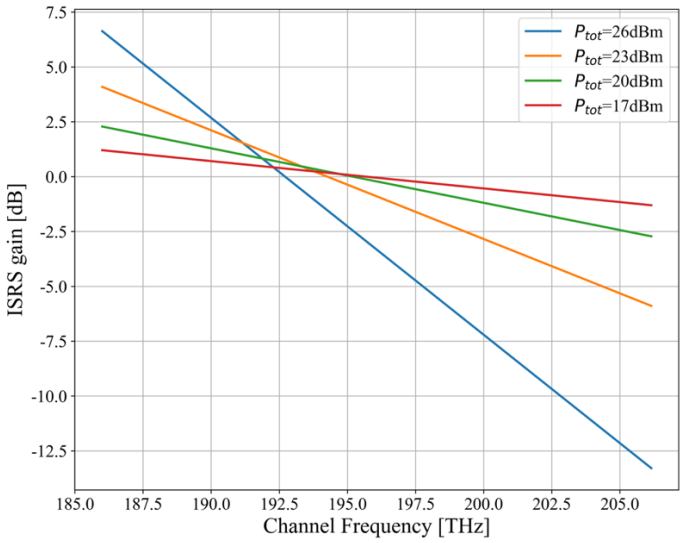

Figure. 1. SRS gain of UWB WDM system after one span 80km transmission under uniform launched power.

2.2. Power control strategy

Due to the influence of SRS gain as shown in Figure 1, in order to ensure the flatness of the ripple at the receiving end, the center frequency power P_{offset} and power slope $Slpoe$ of C-, L-, S- bands are used to control the launched power of each channel. The launched power of channel i is calculated as

$$P_i = P_{offset} + Slope * (f_i - f_{center}) \tag{9}$$

The total channel capacity of the UWB-WDM system is calculated as

$$C = B \cdot log_2(1 + GSNR) \tag{10}$$

Where B is the channel bandwidth, $GSNR$ is defined as $GSNR = \frac{P_{ch}}{P_{ASE}+P_{NLI}}$. In order to maximize channel capacity and ensure ripple flatness, Equation 11 is used as the objective function of the optimization algorithm [14],

$$y = w_1 \frac{N}{\sum_{i=1}^{N} C_i} + w_2\left[\left(C_{max_L} - C_{min_L}\right) + \left(C_{max_C} - C_{min_C}\right) + \left(C_{max_S} - C_{min_S}\right)\right] \tag{11}$$

With w_1 and w_2 are weights of two terms, C_i is the capacity of COI i. By controlling the values of w1 and w2, three different optimization strategies can be implemented. When $w_1 = 1$ and $w_2 = 0$, the maximum channel capacity can be achieved. When $w_1 = 0$ and $w_2 = 1$, the power control with flattest ripple can be achieved. When $w_1 = 1$ and $w_2 = 10$, the power control strategy with flat ripple and large channel capacity can be achieved.

2.3. Optimization algorithm

Marine Predator Algorithm (MPA) is a naturally inspired metaheuristic algorithm proposed by Faramarzi et al. in 2020, which has been widely validated and applied in the optimization of various engineering problems [19]. It is developed

based on two foraging strategies among marine predators: Levy and Brownian movements.

Figure 2 shows the basic strategy of MPA, where the population is divided into $predators$ and $prey$, and the total number of iterations is evenly divided into three phases.

Phase 1 is exploration, where the movement speed is very fast (i.e. with a high step size). The optimal strategy for predators is to remain stationary, while prey undergoes Brownian movements. The updates of step size and position of preys are performed through the following equation,

$$\overrightarrow{stepsize_i} = \overrightarrow{R_B} \otimes \left(\overrightarrow{Elite_i} - \overrightarrow{R_B} \otimes \overrightarrow{Prey_i}\right) \; i = 1, \dots, n$$
$$\overrightarrow{Prey_i} = \overrightarrow{Prey_i} + P.\vec{R} \otimes \overrightarrow{stepsize_i} \tag{12}$$

Where R_B is a vector containing random numbers based on a normal distribution representing Brownian motion. The symbol $\otimes$ means multiplication operations by entry. R is a vector of uniform random number in [0, 1] and $P = 0.5$.

Phase 2 is exploration and development, where predators and prey have a unit speed ratio. At this phase, the preys adopt the Levy movement strategy, while the predator's optimal solution is Brownian movement. Eq. (13) describes the process of prey moment, while Eq. (14) describes the Brownian motion of the predator and the process in which the prey updates its position as predator moves.

$$For\ the\ first\ half\ of\ the\ population$$
$$\overrightarrow{stepsize_i} = \overrightarrow{R_L} \otimes \left(\overrightarrow{Elite_i} - \overrightarrow{R_L} \otimes \overrightarrow{Prey_i}\right) \; i = 1, \dots, n/2$$
$$\overrightarrow{Prey_i} = \overrightarrow{Prey_i} + P.\vec{R} \otimes \overrightarrow{stepsize_i} \tag{13}$$

$$For\ the\ second\ half\ of\ the\ population$$
$$\overrightarrow{stepsize_i} = \overrightarrow{R_B} \otimes \left(\overrightarrow{R_B} \otimes \overrightarrow{Elite_i} - \overrightarrow{Prey_i}\right) \; i = n/2, \dots, n$$
$$\overrightarrow{Prey_i} = \overrightarrow{Elite_i} + P.CF \otimes \overrightarrow{stepsize_i} \tag{14}$$

Where $\overrightarrow{R_L}$ is a vector of random numbers based on Levy distribution of Levy motion, and $CF = \left(1 - \frac{Iter}{Max\_Iter}\right)^{\left(2 \times \frac{Iter}{Max\_Iter}\right)}$ is a parameter that controls the predator's step size, $Iter$ is the current iteration and Max_Iter is the maximum number of iterations.

Phase 3 is at a low-speed ratio, which focuses on high development ability, so predators adopt the Levy strategy. The updates of predators' step size and position are represented by Eq. (15),

$$\overrightarrow{stepsize_i} = \overrightarrow{R_L} \otimes \left(\overrightarrow{R_L} \otimes \overrightarrow{Elite_i} - \overrightarrow{Prey_i}\right) i = 1, \dots, n$$
$$\overrightarrow{Prey_i} = \overrightarrow{Elite_i} + P.CF \otimes \overrightarrow{stepsize_i} \tag{15}$$

In addition, MPA introduces eddy and fish aggregation device (FAD) effects to avoid local optima. When considering FAD as a local optimum, studies have shown that predators spend 80% of their time near FAD and the remaining 20% of their time making longer jumps in different dimensions. Introducing these longer jumps in the simulation process can avoid stagnation at the local optimum.

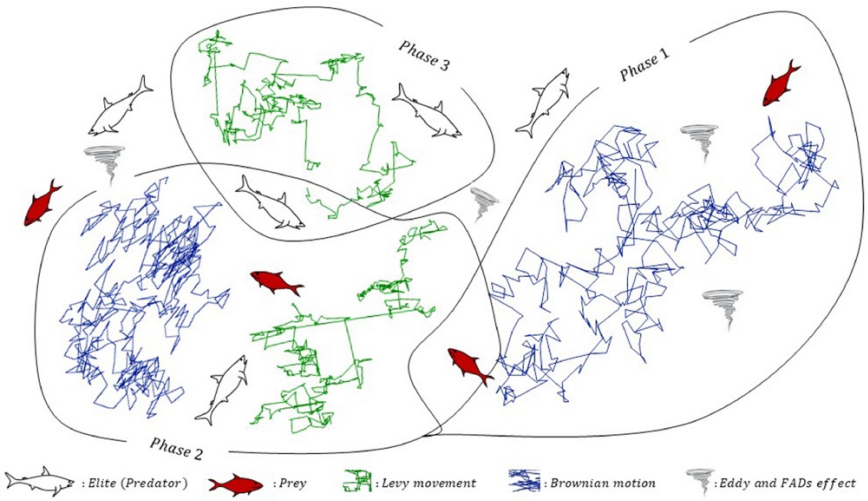

Figure 2. Schematic diagram of MPA optimization process. Phase 1 is exploration, phase 2 is exploration and development, and phase 3 is development. Introduce Eddy and FADs to avoid local optima. [19]

3. SIMULATION RESULTS

3.1. Simulation setup

In this study, a UWB-WDM system covering the C+L+S band was established, with a total of 384 channels, each spanning a length of 80km. Among them, the L-band, C-band, and S-band have 96 channels, 96 channels, and 192 channels, respectively. The protection band between bands is set to 500GHz, and the bandwidth of each channel is 50GHz. Due to the application of the Nyquist WDM system, the symbol rate of the signal is the same as the channel bandwidth, and it is assumed that the noise figure (NF) of OAs over bands is flat. The detailed system parameters are shown in Table 1.

Table I. The main parameters of fiber

Parameters of Fiber	**Values**	**Parameters of Fiber**	**Values**
Loss of L-band (α_l) [dB/km]	0.21	Channel spacing [GHz]	50
Loss of C-band (α_c) [dB/km]	0.20	Bandwidth of guard bands (B_{gb}) [GHz]	500
Loss of S-band (α_s) [dB/km]	0.25	Number of channels	384
Dispersion at 1550 nm (D) [ps/nm/km]	17.0	Optical bandwidth (B_{tot}) [THz]	19.2
Dispersion slope (S) [ps/nm^2/km]	0.091	Reference wavelength [nm]	1454.2
Nonlinear coefficient (γ) [1/W/km]	1.2	Noise figure of L-band (NF_l) [dB]	4.68
Length of span (L_{span}) [km]	80	Noise figure of C-band (NF_c) [dB]	4.25
Symbol rate [Gbaud]	50	Noise figure of S-band (NF_s) [dB]	6.5
Channel bandwidth (B_{ch}) [GHz]	50		

As described in section 2.2., P_{offset} and $Slope$ are used to control the transmission power of each channel, so for the C

-, L -, and S- bands, 6 parameters need to be optimized. The search domain range of $Slope$ is controlled to be -1.5dBm/THz to 1.5dBm/Hz, and the search domain range of P_{offset} being -13dBm to -1dBm. The brute force search (BFS) algorithm with search step sizes of $0.5dBm/THz$ and $2dBm$ for $Slope$ and P_{offset} generated a total of 117649 results, which were used to approximate the global optimum.

3.2. Simulation result

When setting the convergence threshold to 10^{-7} and considering the use of the maximum capacity strategy, the MPA's 5 optimization processes are shown in Figure. 3.(a), and the algorithm will converge after approximately 60 iterations. From Figures. 3. (b) and (c), it can be observed that MPA has a significant advantage in optimization time, completing the optimization in only about 1/25 of BFS's time. Despite adopting the strategy of maximizing capacity, MPA did not pay attention to ripple flatness and still achieved a 2.7Gbps reduction in average ripple compared to BFS. In Figure 4, the optimized channel capacities of BFS and MPA are shown in detail, achieving total capacities of 213.79 Tbps and 214.53 Tbps, respectively. Combined with the results in Figure 3, MPA has advantages over BFS in all aspects and is also more detailed in search granularity.

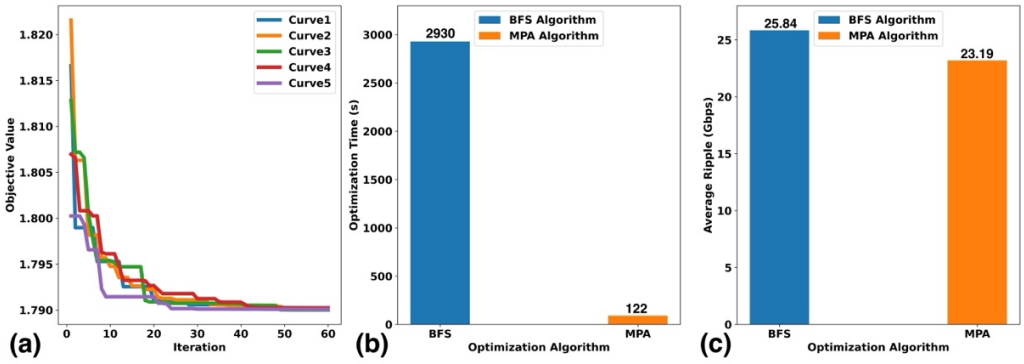

Figure. 3. (a) The convergence process of MPA five time stochastic optimization. (b) Comparison of BFS and MPA optimization time, and (c) Comparison of Ripples between BFS and MPA using maximum capacity strategy.

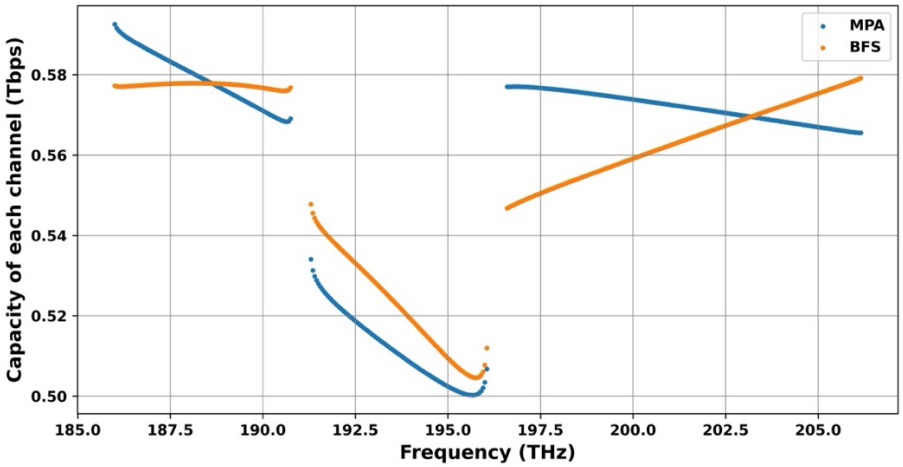

Figure. 4. Comparison of channel capacity after MPA and BFS optimization respectively

In 2.2., three different optimization strategies were designed to control the final optimization scheme. Fig.5. shows the results obtained by applying these three optimization strategies using the MPA algorithm. Among them, Fig.5. (a) and (b) respectively show the optimized input power and capacity per channel for these three strategies. Fig.5. (c) and (d) provide a more intuitive representation of the total capacity and average ripple after optimizing the three strategies. It can be observed that the maximization strategy has the maximum channel capacity (214.53 Tbps), but also the maximum average ripple (23.19 Gbps), which is extremely unfriendly to end users. Relatively speaking, the high-capacity and flat ripple strategy reduces the average ripple to 1.08 Gbps while losing less than 5 Tbps of total capacity, and its performance on both total capacity and average ripple is acceptable. The flattest ripple strategy achieves the lowest average ripple and is the most user-friendly strategy for end-users, but it loses a total capacity of 20 Tbps and 16 Tbps compared to the maximizing strategy and the high-capacity ripple flattening strategy, respectively, which is unacceptable. Overall, the high-capacity and flat ripple strategy achieves a balance between capacity and average ripple, considering both end-user friendliness and maximizing the total system capacity. This strategy can be used in the optimization process of the system.

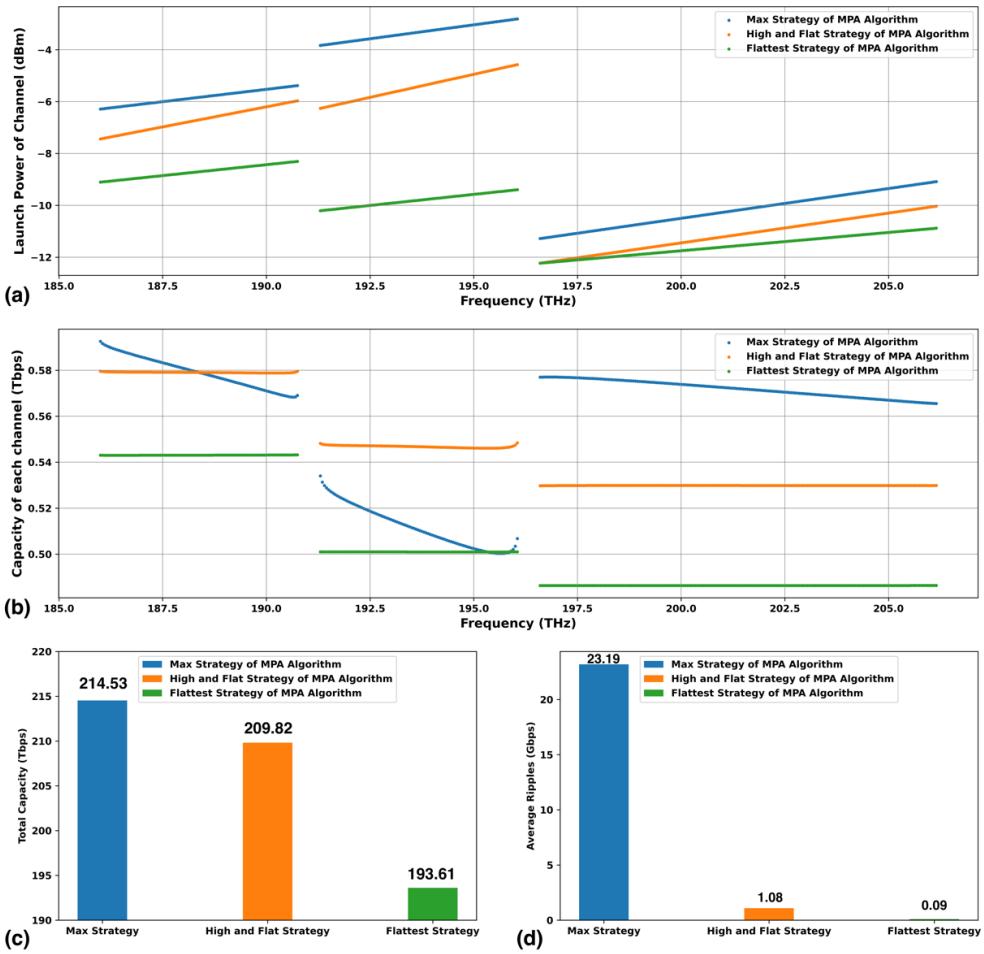

Fig. 5. (a) Optimized launch power of each channel based on three strategies, (b) Capacity of each channel optimized based on three strategies, (c) Total system capacity optimized based on three strategies, and (d) System average ripple optimized based on three strategies.

4. CONCLUSIONS

In this paper, a power control optimization technique based on MPA is proposed. We applied the LOGO strategy and optimized the system using BFS and MPA algorithms respectively. We compared the optimization time, total system capacity, and average ripple of the two algorithms, proving that MPA is leading in all aspects. Meanwhile, in order to balance capacity and ripple, three different power control strategies were adopted for the optimization process of MPA. The results showed that the high-capacity and ripple flat strategy can achieve power flatness at the receiving end with minimal loss of capacity. This study has saved a lot of time in optimizing the launched power of UWB-WDM systems and can adjust the power control strategy as needed.

ACKNOWLEDGEMENTS

Sincere thanks to Professor Yu Changyuan for his guidance on the topic and content of the paper, as well as Dr. Zhong Kangping and Mr. Zhou Jing for their ideas.

REFERENCES

[1] Richardson, D. J., Fini, J. M., & Nelson, L. E. (2013). Space-division multiplexing in optical fibres. Nature photonics, 7(5), 354-362.

[2] H. Ishio, J. Minowa and K. Nosu, "Review and status of wavelength-division-multiplexing technology and its application," in Journal of Lightwave Technology, vol. 2, no. 4, pp. 448-463, August 1984, doi: 10.1109/JLT.1984.1073653.

[3] Ferrari, Alessio, et al. "Power control strategies in C+ L optical line systems." Optical Fiber Communication Conference. Optica Publishing Group, 2019.

[4] Virgillito, Emanuele, et al. "Network performance assessment of C+ L upgrades vs. fiber doubling SDM solutions." Optical Fiber Communication Conference. Optica Publishing Group, 2020.

[5] Virgillito, Emanuele, et al. "Network performance assessment with uniform and non-uniform nodes distribution in C+ L upgrades vs. fiber doubling SDM solutions." 2020 International Conference on Optical Network Design and Modeling (ONDM). IEEE, 2020.

[6] Hamaoka, Fukutaro, et al. "Ultra-wideband WDM transmission in S-, C-, and L-bands using signal power optimization scheme." Journal of Lightwave Technology 37.8 (2019): 1764-1771.

[7] Cantono, Mattia, et al. "On the interplay of nonlinear interference generation with stimulated Raman scattering for QoT estimation." Journal of Lightwave Technology 36.15 (2018): 3131-3141.

[8] Cai, J-X., et al. "94.9 Tb/s single mode capacity demonstration over 1,900 km with C+ L EDFAs and coded modulation." 2018 European Conference on Optical Communication (ECOC). IEEE, 2018.

[9] Hamaoka, Fukutaro, et al. "150.3-tb/s ultra-wideband (s, c, and l bands) single-mode fibre transmission over 40-km using> 519gb/s/a pdm-128qam signals." 2018 European Conference on Optical Communication (ECOC). IEEE, 2018.

[10] Semrau, Daniel, Robert I. Killey, and Polina Bayvel. "The Gaussian noise model in the presence of inter-channel stimulated Raman scattering." Journal of Lightwave Technology 36.14 (2018): 3046-3055.

[11] Semrau, Daniel, Robert I. Killey, and Polina Bayvel. "A closed-form approximation of the Gaussian noise model in the presence of inter-channel stimulated Raman scattering." Journal of Lightwave Technology 37.9 (2019): 1924-1936.

[12] Poggiolini, Pierluigi, et al. "The LOGON strategy for low-complexity control plane implementation in new-generation flexible networks." Optical Fiber Communication Conference. Optica Publishing Group, 2013.

[13] Hamaoka, Fukutaro, et al. "Ultra-wideband WDM transmission in S-, C-, and L-bands using signal power optimization scheme." Journal of Lightwave Technology 37.8 (2019): 1764-1771.

[14] Huaijian Luo, Jianing Lu, Zhuili Huang, Changyuan Yu, and Chao Lu, "Optimization strategy of power control for C+L+S band transmission using a simulated annealing algorithm," Opt. Express 30, 664-675 (2022)

[15] Semrau, Daniel, Robert I. Killey, and Polina Bayvel. "A closed-form approximation of the Gaussian noise model in the presence of inter-channel stimulated Raman scattering." Journal of Lightwave Technology 37.9 (2019): 1924-1936.

[16] D. N. Christodoulides and R. B. Jander, “Evolution of stimulated Raman crosstalk in wavelength division multiplexed systems,” IEEE Photonics Technol. Lett. 8(12), 1722–1724 (1996).

[17] L. B. Djordjevic, A. Stavdas, C. Skoufis, S. Sygletos, and C. Matrakidis, “Analytical modelling of fibre nonlinearities

in amplified dispersion compensated WDM systems," Int. J. Of Model. Simul. 23(4), 226–233 (2003).

[18] Nikita A. Shevchenko, Sam Nallaperuma, and Seb J. Savory, "Maximizing the information throughput of ultra-wideband fiber-optic communication systems," Opt. Express 30, 19320-19331 (2022)

[19] Faramarzi, A., Heidarinejad, M., Mirjalili, S., & Gandomi, A. H. (2020). Marine Predators Algorithm: A nature-inspired metaheuristic. Expert systems with applications, 152, 113377.